Robust High-Accuracy Ultrasonic Range Measurement System

M. M. Saad, Chris J. Bleakley, *Member, IEEE*, and Simon Dobson, *Senior Member, IEEE*

Abstract—This paper presents a novel method for ultrasonic range estimation. The method uses a wideband frequency-hop spread spectrum ultrasonic signal to increase robustness to noise and reverberation. The method applies cross-correlation with earliest peak search and a novel minimum variance search technique to correct the error in the cross-correlation time-of-flight estimate to within one wavelength of the carrier before applying a phase-shift technique for subwavelength range refinement. The method can be implemented digitally in software and only requires low-cost hardware for signal transmission and acquisition. Experimental results show an accuracy of better than 0.5 mm in a typical office environment.

Index Terms—Cross-correlation, frequency-hop spread spectrum (FHSS), phase shift, range estimation, ultrasonic.

I. INTRODUCTION

RANGE measurement is important for many applications, including navigation tools for humans and robots, building mapping, interactive games, resource discovery, asset tracking, and location-aware sensor networking [1]–[8]. Many range measurement techniques have been introduced in the literature, making use of various technologies such as lasers, infrared, radio frequency, and ultrasonic signals [8]–[11]. Of these techniques, ultrasonic signals are distinguished by their capability to estimate range with a high degree of resolution at low cost. Their accuracy is primarily due to the low velocity of ultrasonic wave propagation in air, allowing high accuracy when estimating the signal's propagation distance based on a time-of-flight (TOF) measurement. Errors can occur due to random medium displacements and changes in the speed of sound with humidity and temperature changes in the medium. However, these errors are typically small in indoor environments [8], [30].

Many ultrasonic range measurement methods have been proposed in the literature [12]–[19]. A TOF method is used in most ultrasonic range measurement systems. The TOF method depends on measuring the time taken for an ultrasonic signal to travel between a transmitter and a receiver. The distance between the transmitter and the receiver is then calculated by multiplying the estimated TOF by the acoustic propagation velocity. The delay of the peak of the cross-correlation between the transmitted and received signals can be used to estimate the TOF relative to a radio frequency synchronization signal. Alternatively, a phase-shift method is sometimes used to estimate the distance between the transmitter and the receiver by measuring the phase difference between the transmitted and received signals. The phase-shift method is typically more accurate than the cross-correlation-based TOF method. However, with the phase-shift method, the maximum range that can be estimated is limited to one wavelength of the transmitted signal [15], [17].

This paper proposes a novel method for ultrasonic range estimation. The method uses a wideband frequency-hop spread spectrum (FHSS) ultrasonic signal for robustness to typical signaling impairments, i.e., noise, multipath, and interference from other sources. The method applies cross-correlation TOF estimation with earliest peak search. A novel minimum variance search technique is used to correct errors in the cross-correlation TOF estimate to within one wavelength of the carrier before adding the phase shift for subwavelength range refinement. The accuracy of the method is assessed in simulation and by experiment. The accuracy of the method is shown to exceed that of previously proposed methods. In addition, the method does not require the use of custom measurement circuitry and can be implemented digitally in software.

The rest of this paper is structured as follows: Section II discusses related work. Section III explains the proposed method. Section IV details the experimental method. Simulation and experimental results are provided in Section V. Section VI concludes this paper.

II. RELATED WORK

The single-frequency continuous-wave phase-shift method [12] is the basic technique used to estimate range using an ultrasonic signal with high accuracy. However, the maximum range that can be estimated using this technique alone is limited to one wavelength of the carrier frequency, which means that, at 40 kHz, the maximum range is limited to 8.575 mm, assuming a sound velocity of 343 m/s. Multifrequency continuous-wave phase shifts [13], [14] were used to increase the range by using the difference in phases between frequencies ($\Delta\theta$) and the difference in frequencies (ΔF). However, the maximum range is still limited to $c/\Delta F$, where c is the sound velocity.

In [15], Hua *et al.* applied the phase-shift method to the envelope of an amplitude-modulated (AM) signal. A low-frequency ultrasonic signal modulated by a high-frequency signal with a proper AM index factor is generated. The basic phase-shift method is applied to the received envelope of the AM signal. This extends the range of the system to the wavelength of the lowest frequency used. In the system by Hua *et al.*, the lowest frequency which could be artificially generated was 100 Hz, giving a maximum range of around 3.43 m.

A frequency-change detection and phase-shift method using a binary frequency-shift-keyed signal was proposed in [16]. This technique uses a frequency-change detector to estimate the TOF and refine the estimate by adding the phase shift measured by a digital phase meter. An amplitude change and phase inversion detection and phase-shift method using amplitude- and phase-modulation envelope square waveform was proposed in [17]–[19]. This technique is quite similar to that proposed in [16] except that an amplitude- and phase-change detector is used for TOF estimation instead of a frequency-change detector. The accuracy of these two methods is significantly reduced by the presence of noise. They also need custom analog circuitry with sharp timing synchronization between the transmitter and the receiver.

Of previously proposed digital signal processing (DSP) techniques for TOF estimation, detecting the peak of the cross-correlation between the transmitted and received signals is, in general, more accurate than other techniques such as threshold detection, curve fitting, and sliding window [20]–[22]. However the best resolution that can be achieved using cross-correlation is half the sampling period, meaning that, to obtain higher resolution, a higher sampling frequency must be used. Applying interpolation after the cross-correlation was introduced as a solution to achieving subsample accuracy [23]–[25]. A combined cross-correlation and phase-shift method was proposed in [26], [27], where the cross-correlation is used for the first estimate of the TOF and a phase-shift method is applied to refine the final result to gain better accuracy. This method gives good results when the accuracy of the cross-correlation stage is within one wavelength of the ultrasonic carrier, but if the output of the cross-correlation stage is in error by more than one wavelength of the carrier, then the phase-shift refining stage cannot correct this error and it appears in the final estimate as a significant range error.

Almost all ultrasonic range measurement systems that were previously proposed in the literature use narrowband ultrasonic signals, and have been tested in ideal reverberation-free environments. Narrowband systems are not robust to in-band noise and are highly affected by multipath caused by reflections from walls and surrounding obstacles [28], [29]. Hazas and Ward [29] proposed the use of wideband ultrasonic signaling with direct sequence spread spectrum (DSSS) modulation to improve performance under the conditions of noise and reverberation. In [28], FHSS modulation was shown to provide robustness to multipath and noise and was found to outperform both DSSS and impulsive signaling.

This paper proposes a novel method for ultrasonic range estimation. The method uses a wideband FHSS modulation and applies cross-correlation with earliest peak search and a
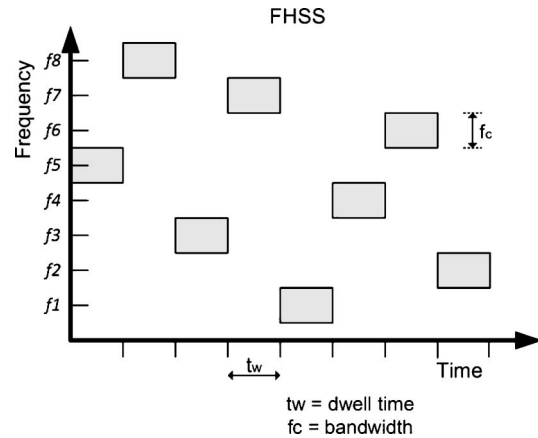

Fig. 1. FHSS.

novel minimum variance search technique to correct errors in the cross-correlation TOF estimate to within one wavelength of the carrier before adding a phase shift for subwavelength range refinement. Compared to previous work on ranging accuracy, the proposed method has the following novel features:

1) wideband ultrasonic signal with FHSS modulation to enhance robustness to multipath and noise;
2) simple cross-correlation with earliest peak search technique to extract the direct path from multipaths;
3) a minimum variance search technique to correct the error in the cross-correlation TOF estimate to within one wavelength of the carrier;
4) easy digital implementation without the need for complex custom analog circuitry.

III. PROPOSED METHOD

The proposed method uses FHSS modulation and a novel algorithm for range estimation. The following sections explain these two points in more detail.

A. FHSS

In FHSS modulation, a carrier hops between a set of frequencies within the available bandwidth. Fig. 1 shows how the carrier hops between different frequencies with time. A pseudo-random sequence determines the frequency-hopping pattern ensuring orthogonality and collision avoidance between signals. The equation that describes the FHSS carrier signal $X^k(t)$ is as follows:

$$X^k(t) = \sin\left(2\pi f^k(t) + \phi\right) \qquad (1)$$

where k denotes user k and $f^k(t)$ is the carrier frequency which is a function of time and the pseudorandom sequence of user k.

Fig. 2 shows the spectrogram of the FHSS signal used in this paper.

B. Range Estimation Algorithm

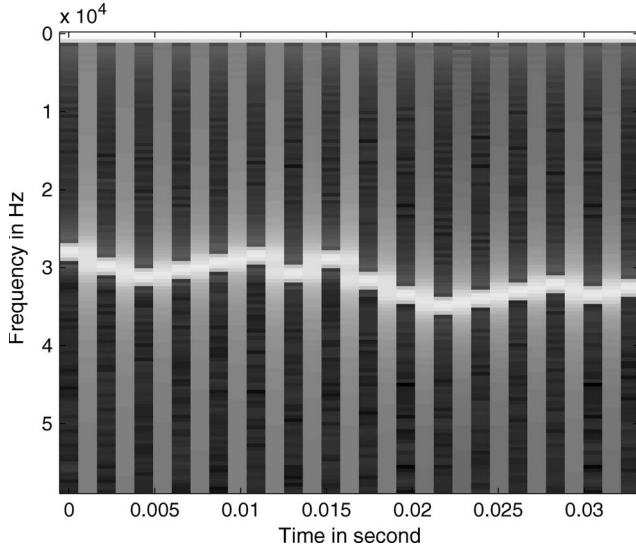Consider an ultrasonic transmitter sending a FHSS signal. The signal is received by a wideband ultrasonic receiver

Fig. 2. Spectrogram of the FHSS signal.

Fig. 3. Cross-correlation between the transmitted and the received signal.

separated by a distance L from the transmitter. The transmitter and the receiver are synchronized, meaning that the receiver is aware of the signal transmission time. Signal acquisition is performed digitally using an analog-to-digital converter (ADC) with a sampling frequency F_s. The proposed method uses the following four procedures to estimate the distance between the transmitter and the receiver:

1) cross-correlation;
2) earliest peak search;
3) phase-shift calculation;
4) minimum variance search.

1) Cross-Correlation: A coarse estimate of the signal TOF between the transmitter and the receiver can be obtained by finding the delay of the earliest peak of the cross-correlation of the received signal with respect to the reference transmitted signal [31]. The TOF is the delay associated with the peak in samples (n_{cross}) multiplied by the sample period ($1/F_s$). The estimated distance between the transmitter and the receiver can be calculated as

$$L_{\text{cross}} = n_{\text{cross}}c/F_s \qquad (2)$$

where c is the propagation speed of sound in air and F_s is the sampling frequency used for signal acquisition. Fig. 3 shows a typical cross-correlation plot where the peak associated with the time delay between the transmitter and the receiver can be clearly seen.

The maximum range that can be estimated using cross-correlation extends as far as the received signal has reasonable signal-to-noise ratio (SNR). The finest time resolution that can be obtained using cross-correlation is limited to $0.5/F_s$. For better resolution, higher sampling rates are required. In addition, the delay of the cross-correlation peak can be in error by one or more samples due to noise.

2) Earliest Peak Search: The peak associated with the correct delay is not always the highest peak. In some cases, the direct path can experience attenuation, giving it a lower cross-correlation peak than indirect multipaths. In other cases, a
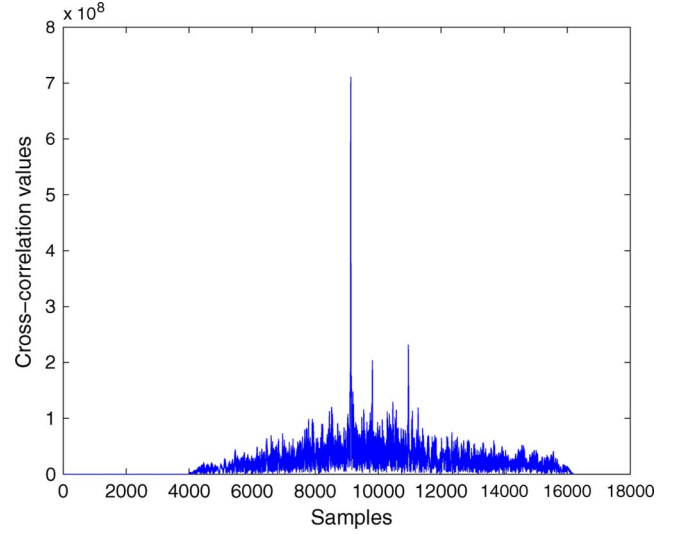
number of indirect paths can combine to produce a peak that is greater than the one associated with the direct path. Herein, a search mechanism is applied to find the earliest arriving cross-correlation peak above the noise floor [30]. The earliest peak is assumed to belong to the direct path that gives the correct TOF. The highest cross-correlation peak is first found, and then, a search back mechanism is applied to search for the earliest peak with amplitude greater than 0.7 of the highest peak. The 0.7 ratio was determined experimentally. It was found to be sufficiently high, so that early peaks are above the noise floor, even at low SNRs, and sufficiently low to guarantee detection of the direct path peak, even with strong reflections.

3) Phase-Shift Calculation: From the previous cross-correlation stage, an estimate for the distance L_{cross} is obtained. The phase shift is used to refine this distance estimate. An error ΔL between the estimated distance L_{cross} and the true distance L is assumed. This error can be written as

$$\Delta L = L - L_{\text{cross}}. \qquad (3)$$

The phase-shift method is used to estimate ΔL with high accuracy and refine the final estimate of the distance L.

Consider that the received signal is

$$y(t) = s(t - L/c) + n(t) \qquad (4)$$

and the known transmitted signal delayed according to L_{cross} is

$$x(t) = s(t - L_{\text{cross}}/c) \qquad (5)$$

where $s(t)$ is the transmitted signal, $n(t)$ is random noise, and c is the sound propagation velocity. The phase shift between $y(t)$ and $x(t)$ gives an estimate of ΔL. This estimated $\hat{\Delta L}$ is then used to refine the final range estimate as follows:

$$\hat{L} = L_{\text{cross}} + \hat{\Delta L}. \qquad (6)$$

Since the FHSS signal's carrier frequency varies with time, a phase shift is calculated for each hop. A cross-spectral density method is used to calculate the phase shift of the received signal $y(t)$ relative to $x(t)$, which is the known transmitted signal

delayed according to L_{cross}. The following equations explain calculation of phase shift for each individual hop [34], [35]:

$$G_{x_m y_m}(\omega) = X_m(\omega)Y_m^*(\omega) \tag{7}$$

where $G_{x_m y_m}$ is the cross-spectral density, ω is the radian frequency which is assumed to be discrete, $X_m(\omega)$ and $Y_m(\omega)$ are the discrete Fourier transforms of the mth hop of $x(t)$ and $y(t)$, respectively, and $*$ denotes the complex conjugate operation.

$G_{xy}(\omega)$ can be related to the transmitted signal $s(t)$ by

$$G_{xy}(\omega) = G_{ss}(\omega)e^{j\omega\tau+\epsilon} \tag{8}$$

where $G_{ss}(\omega)$ is an estimate of the real cross-spectral density of the transmitted signal $s(t)$, τ is the time delay between the two signals $x(t)$ and $y(t)$, and ϵ is the error in phase due to noise and the finite data record.

The estimated phase shift associated with carrier frequency ω_m can be written as

$$\hat{\phi}_m = \text{ang}\,(G_{x_m y_m}(\omega_m)) = \omega_m\tau + \epsilon_m. \tag{9}$$

The standard deviation of the phase estimate is approximated by

$$\sigma[\hat{\phi}_m] \approx \left[\frac{1 - C_{xy}(\omega_m)}{2C_{xy}(\omega_m)}\right]^{1/2} \tag{10}$$

where C_{xy} is the coherence function between $x(t)$ and $y(t)$ defined by

$$C_{xy}(\omega_m) = \frac{|G_{xy}(\omega_m)|^2}{G_{xx}(\omega_m)G_{yy}(\omega_m)}. \tag{11}$$

From $\hat{\phi}_m$ and the sound propagation velocity c, an estimated refinement distance associated with the mth hop $\hat{\Delta L}_m$ can be written as

$$\hat{\Delta L}_m = \frac{\hat{\phi}_m}{\omega_m} * c. \tag{12}$$

Since the value of $\hat{\phi}_m$ is limited to $\pm\pi$, the maximum refinement range that can be achieved by the phase shift without ambiguity is limited to $\pm c/2F_c$, i.e., *half the wavelength* of the carrier frequency.

After calculating $\hat{\Delta L}_m$ for all hops, $\hat{\Delta L}$ can be obtained by averaging $\Delta\hat{L}_m$

$$\hat{\Delta L} = \frac{\sum_{m=0}^{M-1} \hat{\Delta L}_m}{M} \tag{13}$$

where M is the number of hops in the signal.

4) Minimum Variance Analysis: Clearly, the phase-shift method fails when the error in the cross-correlation range estimate is greater than the maximum refinement range which can be achieved by the phase shift, i.e.,

$$|L - L_{cross}| > \lambda/2$$

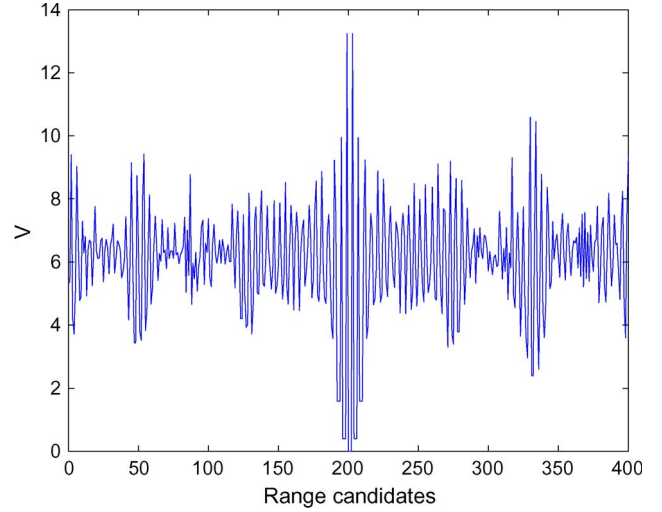where λ is the shortest carrier wavelength.

Fig. 4. Values of phase-shift variance V for 400 range candidates at high SNR (20 dB).

In some cases, L_{cross} is in error by more than $\lambda/2$, particularly in low signal-to-noise and/or high-reverberation scenarios. Hence, we propose to use the variance V of the phase-shift refinement range estimated from different hops as an indicator of the quality of the estimated range L_{cross}

$$V = \sum_{m=0}^{M-1} \frac{\left(\hat{\Delta L} - \hat{\Delta L}_m\right)^2}{M}. \tag{14}$$

In general, V is low when ΔL is less than $\lambda/2$, as $\hat{\Delta L}_m$ estimated over different hops will provide consistent estimates of ΔL. When ΔL is greater than $\lambda/2$, V is large due to variations in $\hat{\Delta L}_m$ estimated at different hops. Hence, the value of V can be used to check whether ΔL is smaller than $\lambda/2$.

An iterative procedure is used to search across a number of candidate range estimates; for each candidate, the phase-shift refinements $\hat{\Delta L}_m$ are obtained and used to determine $\hat{\Delta L}$ and V. The candidate range with minimum V is selected as the correct range estimate. The candidate ranges are integer sample delays in a window of length $(L_w + 1)$ centered on the delay associated with the cross-correlation peak

$$L_{\text{cross}} - L_w/2 : L_{\text{cross}} + L_w/2.$$

Fig. 4 shows the values of V for a window of 400-sample length. The minimum value of V which is associated with the correct range candidate is clearly observed. Fig. 5 shows the values of V for the same window in the case of low SNR (SNR $= -10$ dB). Despite the noise, the candidate with the minimum variance is still clear.

5) Summary: The following pseudocode explains the overall range estimation algorithm:

R_{xy}: Cross-correlate the received signal with the transmitted signal.

L_{cross}: Find the range candidate associated with the earliest arriving cross-correlation peak.
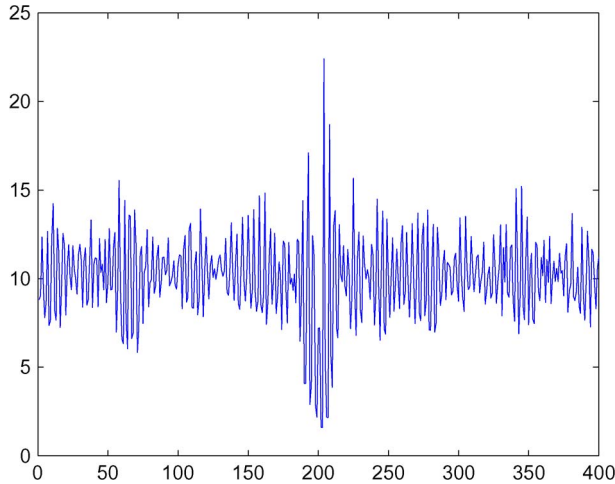
L_w: Define the candidate window length.

Fig. 5. Values of phase-shift variance V for 400 range candidates at low SNR (-10 dB).

for $l = L_{\text{cross}} - L_w/2 : L_{\text{cross}} + L_w/2$ **do**
　　for $m = 0$ to $M - 1$ **do**
　　　　Calculate $\hat{\Delta} L_m$.
　　end for
　　Calculate V_l.
　　Calculate $\hat{\Delta} L$.
end for
l_{correct}: Find the range candidate associated with the minimum value of V.
$\hat{L}$: Calculate the final refined range estimate.

IV. EXPERIMENTAL METHOD

The range estimation algorithm was implemented in software using Matlab and simulated prior to experiments. The image method [32] was used to obtain synthetic impulse responses for a 4 m × 4 m × 4 m room with reflection coefficients for walls, ceiling, and floor equal to 0.6 and an SNR equal to 20 dB, unless otherwise stated. An FHSS signal was designed with 16 frequency slots in the band between 28 and 36 kHz with 460 Hz separation between adjacent frequencies. The signal consists of 16 hops; each hop occupies a time slot of 2.2 ms.

Actual experiments were performed using the same signal applied in a prototype range measurement system. The transmitters used were Prowave 250ST180 piezoelectric transducers [33] which have a bandwidth of 2 kHz, centered at 41 kHz. A bandwidth expansion circuit giving a useable bandwidth of 30 kHz was used to support wideband modulation [34]. SPM0204 ultrasonic sensors were used as receivers [35]. These microphones, based on capacitive micromachined ultrasonic transducer technology, have nearly a flat response between 10 and 70 kHz. A DSP board from Sundance, model 361A, was used for signal acquisition [36]. It includes a C6416 DSP from Texas Instruments with two daughter boards, an SMT377 with eight independent digital-to-analog converters, and an SMT317 with an eight-channel ADC. Coaxial cables were used to connect the daughter cards to the transmitter and receiver boards. The sampling frequency used was 117.5 kHz, which is the lowest sampling frequency greater than $2F_c$ provided
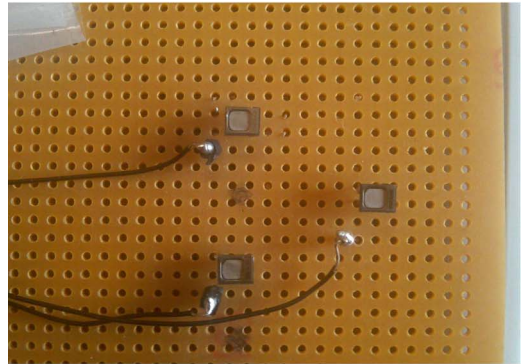
Fig. 6. Photographs of experimental setup. (a) Office room. (b) Transmitter. (c) Receivers.

by the DSP board hardware. F_c is assumed to be equivalent to the highest carrier frequency among the FHSS frequency slots. The carrier frequencies are determined by the bandwidth of the ultrasonic transducer and the FHSS signal design. The value of F_c in these experiments was 36 kHz. The experimental system was installed in a typical office room with dimensions 350 cm × 285 cm × 270 cm. The sound velocity was assumed to be constant during the experiments. The effects of variation in temperature and humidity on sound velocity were assumed to be negligible as the measurement was taken over a short period of time. Fig. 6 shows photographs of the experimental system setup.

V. RESULTS

In order to evaluate the performance of the proposed method, simulation and experimental results were obtained.

TABLE I
PERCENTAGE OF ERRORS GREATER THAN $\lambda/2$ USING
CROSS-CORRELATION WITH AND WITHOUT EARLIEST
PEAK SEARCH (REFLECTION COEFFICIENT = 0.7)

SNR in dB	20	10	5	0	-5	-10	-12
Without earliest peak search	13%	14%	17%	21%	26%	33%	40%
With earliest peak search	0%	2%	5 %	11%	15%	25%	36%
Improvement	13%	12%	12%	10%	11%	8%	4%

TABLE II
PERCENTAGE OF ERRORS GREATER THAN $\lambda/2$ USING
CROSS-CORRELATION WITH AND WITHOUT EARLIEST
PEAK SEARCH (SNR = 0 dB)

Reflection Coefficient	0	0.2	0.4	0.6	0.7	0.8	0.9
Without earliest peak search	9%	11%	13%	18%	21%	23%	30%
With earliest peak search	9%	8%	9%	11%	11%	10%	14%
Improvement	0%	3%	4%	7%	10%	13%	16%

TABLE III
PERCENTAGE OF ERRORS GREATER THAN 0.5 mm USING THE PROPOSED
METHOD WITH AND WITHOUT MINIMUM VARIANCE SEARCH
(REFLECTION COEFFICIENT = 0.7)

SNR in dB	20	10	5	0	-5	-10	-12
Without minimum variance search	4%	7%	10%	18%	18%	28%	55%
With minimum variance search	0%	1%	2%	2%	4%	21%	41%
Improvement	4%	6%	8%	16%	14%	7%	14%

A. Simulation Results

An ultrasonic transmitter sending the FHSS signal described in Section III was located at the corner of the room. The receiver was moved between 400 different locations in the room, and in each location, the received signal was processed and the range to the transmitter was estimated using the proposed algorithm. The simulation was run 100 times for each location, and an estimate was obtained for each simulation run, giving a total of 40 000 estimates.

Table I shows that the proposed earliest peak search technique improves the range estimates for various SNRs. It compares the percentages of errors greater than $\lambda/2$ when estimating the range using cross-correlation only and cross-correlation with earliest peak search.

Table II shows that the proposed earliest peak search technique improves the range estimates for various reflection coefficients. It compares the percentages of errors greater than $\lambda/2$ when estimating the range using cross-correlation only and cross-correlation with earliest peak search.

Table III shows that the proposed minimum variance search technique improves the range estimates for various SNRs. It compares the percentages of errors greater than 0.5 mm when estimating the range using cross-correlation with earliest peak and phase shift without minimum variance search, and cross-correlation with earliest peak and phase shift with minimum variance search.

Table IV shows that the proposed minimum variance search technique improves the range estimates for various reflection coefficients. It compares the percentages of errors greater than 0.5 mm when estimating the range using cross-correlation with earliest peak and phase shift without minimum variance search, and cross-correlation with earliest peak and phase shift with minimum variance search.

TABLE IV
PERCENTAGE OF ERRORS GREATER THAN 0.5 mm USING THE
PROPOSED METHOD WITH AND WITHOUT MINIMUM
VARIANCE SEARCH (SNR = 0 dB)

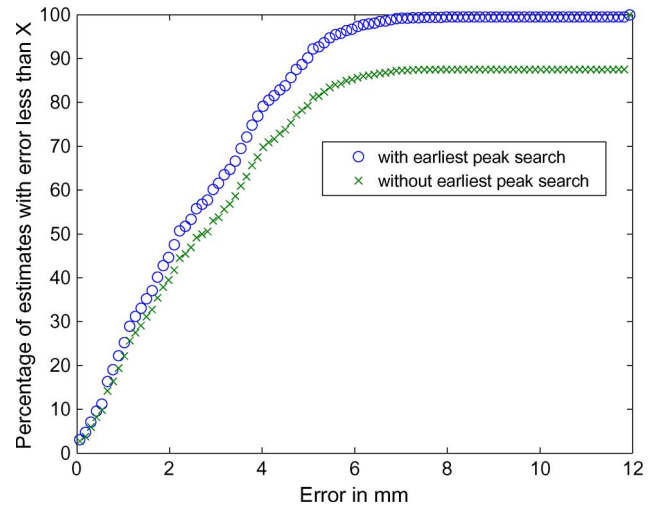| Reflection Coefficient	0	0.2	0.4	0.6	0.7	0.8	0.9
Without minimum variance search	9%	9%	9%	14%	18%	18%	24%
With minimum variance search	0%	0%	1%	1%	2%	6%	14%
Improvement	9%	9%	8%	13%	16%	12%	10%

Fig. 7. Cumulative error of the estimated range using cross-correlation with and without earliest peak search.
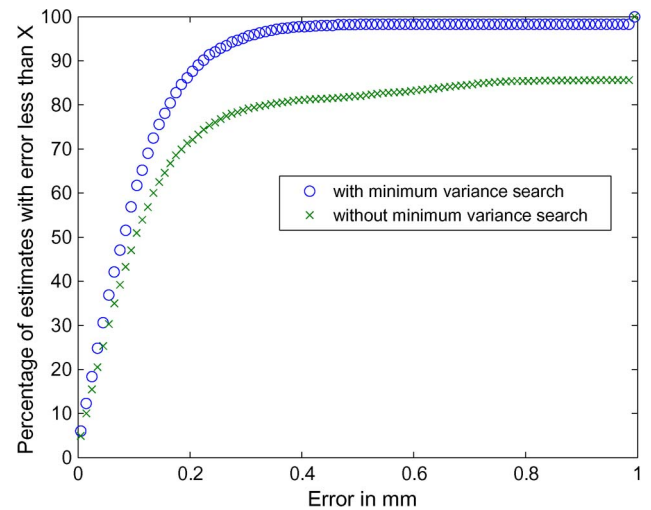

Fig. 8. Cumulative error of the estimated ranges using the proposed method with and without minimum variance search.

Fig. 7 shows the cumulative error of the estimated ranges using cross-correlation only and cross-correlation with earliest peak search for all 40 000 estimates when SNR = 0 dB and reflection coefficient = 0.7. Fig. 8 shows the cumulative error of the estimated ranges using cross-correlation with earliest peak and phase shift and when using cross-correlation with earliest peak and phase shift with minimum variance search for all 40 000 estimates when SNR = 0 and reflection coefficients = 0.7. Comparing Figs. 7 and 8, the improvement due to the incorporation of phase shift can be seen (note the different

TABLE V
RMSE AND STANDARD DEVIATION VERSUS SNR

	SNR in dB	-10	-8	-6	-4	0	2	5	10
RMSE mm	PM	3.84	2.97	2.76	2.43	1.58	0.82	0.17	0.13
	CC-INT	3.86	3.43	3.38	3.17	2.84	2.60	2.47	2.25
	CC	3.94	3.54	3.23	3.37	3.11	2.87	2.84	2.71
σ mm	PM	3.83	2.96	2.69	2.40	1.56	0.81	0.13	0.03
	CC-INT	3.84	3.40	3.23	3.13	2.71	2.35	1.93	1.15
	CC	3.91	3.48	3.37	3.30	2.94	2.59	2.24	1.59

TABLE VI
RMSE AND STANDARD DEVIATION VERSUS NUMBER
OF ACTIVE TRANSMITTERS

NT	1	2	3	4	5	6
RMSE mm	0.11	0.23	0.46	0.73	1.04	1.38
σ mm	0.01	0.01	0.28	0.59	0.87	1.17

TABLE VII
RMSE AND STANDARD DEVIATION VERSUS RANGE

| Range m	0.5	1	2	4	5	6	7
RMSE mm	0.018	0.021	0.104	0.630	0.876	1.276	1.894
σ mm	0.007	0.012	0.058	0.630	0.876	1.274	1.894

Fig. 9. Cumulative error of the estimated ranges using the proposed method.

TABLE VIII
STANDARD DEVIATION VERSUS NUMBER OF ACTIVE TRANSMITTERS

NT	1	2	3
σ mm	0.1619	0.3140	0.5392

x-axes). Simulations show that the proposed system provides an accuracy of 0.2 mm in 90% of the cases. These results show the improved accuracy of the proposed method and illustrate its robustness to noise and multipath.

Controlled experiments were carried out to evaluate the performance of the proposed method and to compare it with other methods. Table V compares the standard deviation (σ) and the root-mean-square error (rmse) obtained using the proposed method (PM) with that obtained using cross-correlation with interpolation (including earliest peak search) (CC-INT), and cross-correlation alone (including earliest peak search) (CC). SNR has been varied between -10 and 10 dB, while the reflection coefficient was fixed to 0.7. For each SNR value, 1000 simulation runs were performed. Results show that the proposed method (PM) outperforms other methods over a range of SNR values. Moreover, it shows that the accuracy of the proposed method is very good at high SNR.

The accuracy of the proposed method was tested in the presence of other interfering sources using the same FHSS scheme. In the simulation, up to six transmitters sending different FHSS patterns were placed equidistant from the receiver in a 4 m × 4 m × 4 m room with reflection coefficients for walls, ceiling, and floor equal to 0.65 and an SNR equal to 20 dB. The number of simultaneously active transmitters was varied from 1 to 6, and 1000 simulation runs were performed for each case. Table VI shows the values of the standard deviation (σ) and the RMSE obtained versus the number of active transmitters (NT). Results show that the proposed method is robust to interfering sources. Accuracy degrades somewhat when the number of transmitters increases, but even so, the overall accuracy is good.

The accuracy of the proposed method was tested over various distances. The SNR was 20 dB at 0.5 m distance from the transmitter. Table VII shows the values of the standard deviation (σ) and the root-mean-square error (RMSE) obtained from 1000 runs versus the distances between the transmitter and the receiver (from 0.5 to 7 m). Results show that the proposed method has a reasonable accuracy over a large range of source–receiver separations. Accuracy decreases slightly as separation increases. This is due to signal attenuation with distance, which causes degradation in the SNR.
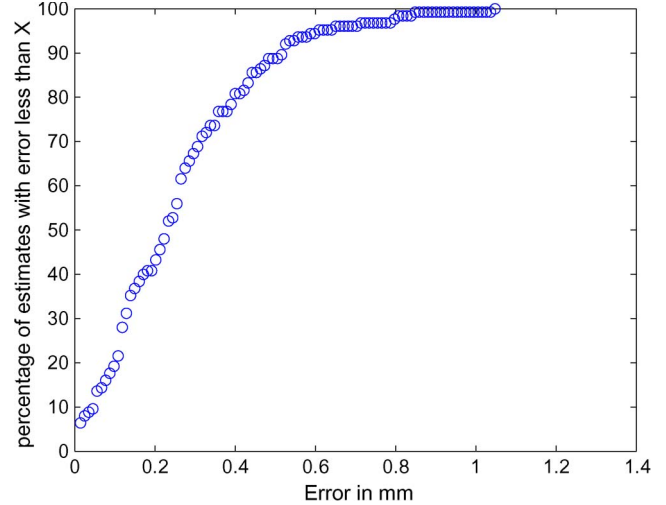
B. Experimental Results

Three receiver sensors were fixed on a printed circuit board, and the distance between them was measured with high accuracy. A transmitter was moved between three different locations, while the receiver board remained stationary. The ranges between the transmitter and the receiver board were 2.1, 2.3, and 2.5 m for locations 1, 2, and 3, respectively. A total of 125 range estimates from each individual sensor were obtained. Due to the lack of sophisticated tools to measure the true range between the transmitter and the receiver with sufficient accuracy, the differences between the estimated ranges to the three receivers were calculated by subtracting the estimated ranges for each pair of sensors. The estimated range differences were compared with the sensor physical separation measured with a micrometer, allowing for angle of arrival. Fig. 9 shows that the error is less than 0.5 mm in 90% of the cases. The error is double the simulation results due to the subtraction of two estimates.

The receiver was separated by 1 m from the transmitter, and 100 estimates were obtained. The standard deviation of the estimates was 0.1619 mm. A second transmitter sending a different FHSS signal was located facing the receiver and separated by 1 m from it. The standard deviation of the estimates when the two transmitters were sending simultaneously was 0.3140 mm. The same experiment was repeated with three transmitters, and the standard deviation this time was 0.5392 mm. Table VIII summarizes the previous results. These results show that the proposed method is accurate and robust to other interfering sources.

VI. Conclusion

A novel method for range measurement using FHSS ultrasonic signals combining cross-correlation and phase-shift methods has been developed. The method picks the earliest peak in the cross-correlation of the received signal with the transmitted reference signal to obtain a first estimate of the range. A novel minimum variance search technique is applied to correct the error in the cross-correlation TOF estimate to within one wavelength of the carrier before applying a phase shift for subwavelength range refinement. The simulation results show the robustness of the method to noise and multipath. The method was experimentally tested using low-cost hardware and software in a typical office environment, and it provides an accuracy of better than 0.5 mm in 90% of cases.

References

[1] J. Broadbent and P. Marti, "Location aware mobile interactive guides: Usability issues," in *Proc. 4th ICHIM*, 1997, pp. 162–172.

[2] D. Moore, J. Leonard, D. Rus, and S. Teller, "Robust distributed network localization with noisy range measurements," in *Proc. 2nd Int. Conf. Embedded Netw. Sensor Syst.*, 2004, pp. 50–61.

[3] A. Patil, J. Munson, D. Wood, and A. Cole, "Bluebot: Asset tracking via robotic location crawling," *Comput. Commun.*, vol. 31, no. 6, pp. 1067–1077, Apr. 2008.

[4] O. Rashid, I. Mullins, P. Coulton, and R. Edwards, "Extending cyberspace: Location based games using cellular phones," *Comput. Entertainment (CIE)*, vol. 4, no. 1, p. 4, Jan. 2006.

[5] D. Hahnel, D. Schulz, and W. Burgard, "Map building with mobile robots in populated environments," in *Proc. IEEE/RSJ Int. Conf. IROS*, 2002, pp. 496–501.

[6] M. Bosse, P. Newman, J. Leonard, and S. Teller, "Simultaneous localization and map building in large-scale cyclic environments using the Atlas framework," *Int. J. Robot. Res.*, vol. 23, no. 12, pp. 1113–1139, Dec. 2004.

[7] A. Harter, A. Hopper, P. Steggles, A. Ward, and P. Webster, "The anatomy of a context-aware application," *Wirel. Netw.*, vol. 8, no. 2, pp. 187–197, Mar.–May 2002.

[8] J. Hightower and G. Borriello, "Location systems for ubiquitous computing," *Computer*, vol. 34, no. 8, pp. 57–66, Aug. 2001.

[9] K. Whitehouse, C. Karlof, and D. Culler, "A practical evaluation of radio signal strength for ranging-based localization," *ACM SIGMOBILE Mobile Comput. Commun. Rev.*, vol. 11, no. 1, pp. 41–52, Jan. 2007.

[10] C. Yuzbasioglu and B. Barshan, "Improved range estimation using simple infrared sensors without prior knowledge of surface characteristics," *Meas. Sci. Technol.*, vol. 16, no. 7, pp. 1395–1409, Jul. 2005.

[11] M. Amann, T. Bosch, M. Lescure, R. Myllyla, and M. Rioux, "Laser ranging: A critical review of usual techniques for distance measurement," *Opt. Eng.*, vol. 40, no. 1, pp. 10–19, Jan. 2001.

[12] F. Figueroa and E. Barbieri, "An ultrasonic ranging system for structural vibration measurements," *IEEE Trans. Instrum. Meas.*, vol. 40, no. 4, pp. 764–769, Aug. 1991.

[13] K. Huang and Y. Huang, "Multiple-frequency ultrasonic distance measurement using direct digital frequency synthesizers," *Sens. Actuators A, Phys.*, vol. 149, no. 1, pp. 42–50, Jan. 2009.

[14] C. Huang, M. Young, and Y. Li, "Multiple-frequency continuous wave ultrasonic system for accurate distance measurement," *Rev. Sci. Instrum.*, vol. 70, no. 2, pp. 1452–1458, Feb. 1999.

[15] H. Hua, Y. Wang, and D. Yan, "A low-cost dynamic range-finding device based on amplitude-modulated continuous ultrasonic wave," *IEEE Trans. Instrum. Meas.*, vol. 51, no. 2, pp. 362–367, Apr. 2002.

[16] S. Huang, C. Huang, K. Huang, and M. Young, "A high accuracy ultrasonic distance measurement system using binary frequency shift-keyed signal and phase detection," *Rev. Sci. Instrum.*, vol. 73, no. 10, pp. 3671–3677, Oct. 2002.

[17] Y. Huang, J. Wang, K. Huang, C. Ho, J. Huang, and M. Young, "Envelope pulsed ultrasonic distance measurement system based upon amplitude modulation and phase modulation," *Rev. Sci. Instrum.*, vol. 78, no. 6, p. 065 103, Jun. 2007.

[18] Y. Huang and M. Young, "An accurate ultrasonic distance measurement system with self temperature compensation," *Instrum. Sci. Technol.*, vol. 37, no. 1, pp. 124–133, Jan. 2009.

[19] K. Sasaki, H. Tsuritani, Y. Tsukamoto, and S. Iwatsubo, "Air-coupled ultrasonic time-of-flight measurement system using amplitude-modulated and phase inverted driving signal for accurate distance measurements," *IEICE Electron. Exp.*, vol. 6, no. 21, pp. 1516–1521, 2009.

[20] B. Barshan, "Fast processing techniques for accurate ultrasonic range measurements," *Meas. Sci. Technol.*, vol. 11, no. 1, pp. 45–50, Jan. 2000.

[21] M. Parrilla, J. Anaya, and C. Fritsch, "Digital signal processing techniques for high accuracy ultrasonic range measurements," *IEEE Trans. Instrum. Meas.*, vol. 40, no. 4, pp. 759–763, Aug. 1991.

[22] G. Andria, F. Attivissimo, and N. Giaquinto, "Digital signal processing techniques for accurate ultrasonic sensor measurement," *Measurement*, vol. 30, no. 2, pp. 105–114, Sep. 2001.

[23] D. Marioli, C. Narduzzi, C. Offelli, D. Petri, E. Sardini, and A. Taroni, "Digital time-of-flight measurement for ultrasonic sensors," *IEEE Trans. Instrum. Meas.*, vol. 41, no. 1, pp. 93–97, Feb. 1992.

[24] R. Queirós, R. Martins, P. Girão, and Serra, "A new method for high resolution ultrasonic ranging in air," in *Proc. XVIII IMEKO World Congr. Metrol. Sustainable Develop.*, 2006.

[25] L. Svilainis and V. Dumbrava, "The time-of-flight estimation accuracy versus digitization parameters," *Ultragarsas (Ultrasound)*, vol. 63, no. 1, pp. 12–17, 2008.

[26] F. Gueuning, M. Varlan, C. Eugene, and P. Dupuis, "Accurate distance measurement by an autonomous ultrasonic system combining time-of-flight and phase-shift methods," in *Proc. IEEE IMTC*, 1996, vol. 1, pp. 399–404.

[27] R. Queiros, P. Girao, and A. Cruz Serra, "Cross-correlation and sine-fitting techniques for high resolution ultrasonic ranging," in *Proc. IEEE IMTC*, 2006, pp. 552–556.

[28] J. Gonzalez and C. J. Bleakley, "Accuracy of spread spectrum techniques for ultrasonic indoor location," in *Proc. 15th Int. Conf. Digital Signal Process.*, 2007, pp. 284–287.

[29] M. Hazas and A. Ward, "A novel broadband ultrasonic location system," in *Proc. UbiComp*, 2002, pp. 299–305.

[30] L. Girod and D. Estrin, "Robust range estimation using acoustic and multimodal sensing," in *Proc. IEEE/RSJ Int. Conf. IROS*, 2001, pp. 1312–1320.

[31] D. Sarwate and M. Pursley, "Crosscorrelation properties of pseudorandom and related sequences," *Proc. IEEE*, vol. 68, no. 5, pp. 593–619, May 1980.

[32] J. Allen and D. Berkley, "Image method for efficiently simulating small-room acoustics," *J. Acoust. Soc. Amer.*, vol. 65, no. 4, pp. 943–950, Apr. 1979.

[33] [Online]. Available: http://www.piezotechnologies.com/

[34] J. Gonzalez and C. Bleakley, "Robust high precision ultrasonic 3D location for ubiquitous computing," Ph.D. dissertation, Univ. College Dublin, Dublin, Ireland, 2010.

[35] [Online]. Available: http://www.elfaelektronika.lt/artnr/30-104-44/ultrasonic-sensor-forsurface- mounting-smd

[36] [Online]. Available: http://www.sundancedsp.com/